Copper enhanced (111) texture in silver thin films on amorphous Si O 2

Yeongseok Zoo, H. Han, and T. L. Alford

Citation: Journal of Applied Physics **102**, 083548 (2007); doi: 10.1063/1.2800998
View online: http://dx.doi.org/10.1063/1.2800998
View Table of Contents: http://scitation.aip.org/content/aip/journal/jap/102/8?ver=pdfcov
Published by the AIP Publishing

Copper enhanced (111) texture in silver thin films on amorphous SiO_2

Yeongseok Zoo,[a] H. Han, and T. L. Alford[b]
School of Materials, Arizona State University, Tempe, Arizona 85287-8706, USA

(Received 3 April 2007; accepted 31 August 2007; published online 31 October 2007)

Small amounts (5 at. %) of copper were added to silver thin films to improve adhesion and minimize agglomeration on SiO_2 layers. Resistivity measurements from the Ag(Cu) films showed that small Cu additions do not significantly increase the resistivity compared to pure Ag. Texture evolution and surface morphology of Ag and Ag(Cu) thin films on SiO_2 were also investigated using x-ray diffraction (XRD) techniques and atomic force microscopy. Normalized (111) θ-2θ XRD intensities increased from 91.6% to 96.8% upon addition of Cu, likely due to enhanced adatom diffusion resulting from the Cu addition. XRD pole figure analysis revealed differences in texture evolution between the Ag and Ag(Cu) thin films. Since high adatom surface diffusion of Cu promotes preferred grain growth of the Ag matrix, Ag(Cu) thin films showed enhanced (111) texture compared to Ag thin films. Glancing angle XRD results confirmed the evolution of (111) texture in the Ag and Ag(Cu) thin films. In the case of Ag, (111) texture was enhanced mainly by recrystallization of disordered regions during annealing. In addition to recrystallization, (111) texture enhancement in Ag(Cu) was attributed to consumption of grains with other non-(111) crystallographic orientations. © *2007 American Institute of Physics*. [DOI: 10.1063/1.2800998]

I. INTRODUCTION

As electronic devices are further miniaturized, the microstructure and texture evolution of thin films during thermal processing are of particular interest because they are directly related to reliability of the metallization.[1–4] For metal interconnects used in integrated circuits, electromigration has been recognized as a key factor limiting the performance of devices under high current stresses.[5,6] Electromigration resistance is strongly dependent on the microstructure of thin metal films, due to the fact that mass transport during electromigration occurs primarily along grain boundaries of the thin films. It has been reported that a "bamboo" structure enhances the electromigration resistance of metallic lines.[7] Large mean grain sizes and preferred-oriented grains can improve the electromigration reliability of thin films.[8,9] For these reasons, grain growth and texture evolution of Al and Cu thin films have been investigated extensively for a variety of film thicknesses,[10] deposition conditions,[11] and substrate types.[12]

Silver has potential for ultralarge-scale integration applications due to the fact that it has the lowest bulk electrical resistivity of pure metals and higher electromigration resistance than other interconnect materials.[10,13] However, agglomeration during thermal processing limits the stability of Ag thin films and compromises the film's reliability. Kim *et al.*[14] reported that the agglomeration of Ag thin films can be significantly reduced by the addition of Al since Ag(Al) alloys form a self-passivating Al oxide on the surface. However, Al addition decreased the preferred orientation of the Ag thin films.[14]

In this study, the texture evolution of Ag thin films was investigated as a function of annealing temperature and was compared to the texture evolution in Ag(Cu) alloy films under the same annealing conditions. In addition, surface morphologies were compared using atomic force microscopy (AFM). Based on the results, we discuss the [111] preferred orientation of Ag(Cu) thin films and attribute the texture to the presence of Cu. The preferred orientation can result in improved electromigration resistance over pure Ag.

II. EXPERIMENTAL DETAILS

Silver and silver-copper thin films were deposited on thermally grown SiO_2 using electron-beam evaporation. Typical base and deposition pressures were 3×10^{-6} and 4.7×10^{-6} Torr, respectively. The samples were annealed in vacuum (base pressure $\sim10^{-8}$ Torr) for 1 h at various temperatures (300, 400, 500, and 600 °C) in order to investigate texture changes as a function of annealing temperature. Resistivities of Ag and Ag(Cu) films were measured using a typical in-line four-point probe configuration.[13,14]

Texture evolution of the Ag and Ag(Cu) thin films was investigated by Bragg-Brentano configuration (θ-2θ geometry) and pole figure analyses. Conventional θ-2θ x-ray diffraction (XRD) scans provided relative intensities of (111) and (200) peaks for planes parallel to the surface of the substrate. Texture along the film normal was evaluated by comparison of the intensities of x rays diffracted from each $\{hkl\}$ plane. Pole figure analysis provided spatial texture information for specific sets of planes as a function of sample tilt angle (ψ). The texturing of (111) and (200) planes were measured while varying tilt angle from 0° to 85°.[14]

Glancing angle x-ray diffraction analysis was used to investigate the thermal behavior of the Ag grains. Figure 1 shows the geometry used for glancing incident angle x-ray diffraction. For the case of a symmetrical diffraction technique, as in the case of Bragg-Brentano configuration, the angle of incidence is always equal to the exit angle. If the

[a]Electronic mail: zooys94@asu.edu
[b]Electronic mail: alford@asu.edu

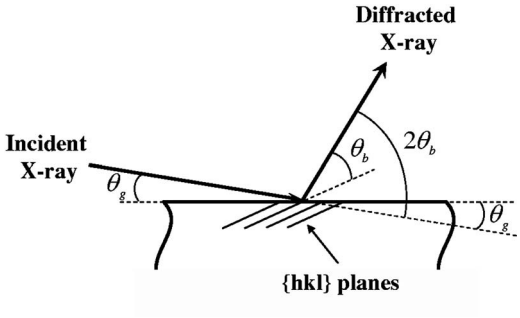

FIG. 1. Schematic of glancing incident angle x-ray diffraction geometry.

diffractometer moves to a higher angle for detecting high {*hkl*} reflections, the penetration depth of x rays may be greater than the thickness of the thin film, resulting in unwanted substrate peaks and increased background noise. The glancing angle geometry sets the incident beam at a low angle (i.e., 1°) to maximize the x-ray interaction volume in the thin film while the detector is moved through a desired 2θ range. The resulting configuration is asymmetric and the detected {*hkl*} planes are tilted by specific angles with respect to the surface normal.

Surface images of the Ag and Ag(Cu) thin films were obtained with acoustic-mode AFM using a Molecular Imaging Pico scanning-probe microscopy (SPM) system. The images were compared to study the impact of Cu on surface and texture evolution of the Ag thin films.

III. RESULTS AND DISCUSSION

Resistivity changes in Ag and Ag(Cu) thin films as a function of annealing temperature are shown in the Fig. 2. For as-deposited thin films, the resistivity of the Ag(Cu) film is slightly higher than that of the Ag film due to resistivity changes arising from Cu addition (scattering from Cu solute).[15] When the sample is annealed, however, the resistivities of the Ag and Ag(Cu) thin films become similar. The resistance values are stable up to 600 °C. The resistivities of both samples increase abruptly at 700 °C, likely due to a discontinuous conduction path resulting from agglomeration

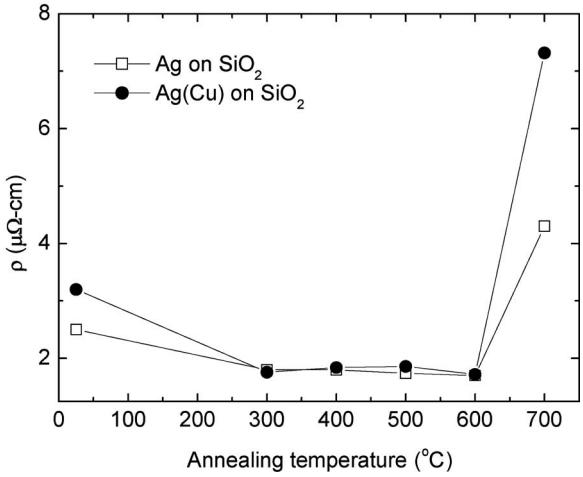

FIG. 2. Electrical resistivity of Ag and Ag(Cu) thin films on SiO_2 layer as a function of annealing temperature.

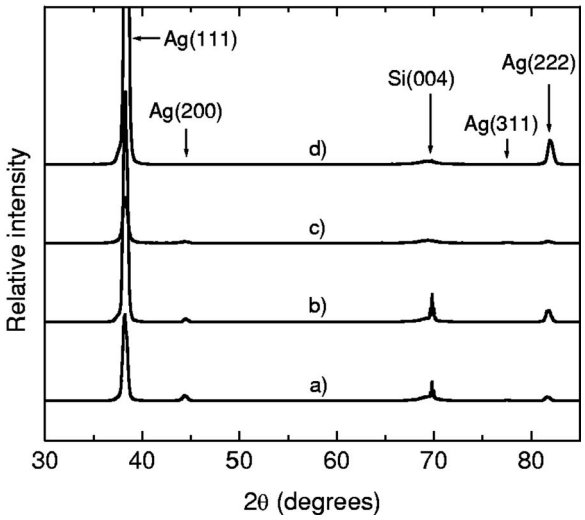

FIG. 3. Bragg-Brentano XRD scans obtained from Ag and Ag(Cu) thin films on SiO_2 layers: (a) Ag as deposited, (b) Ag annealed at 600 °C, (c) Ag(Cu) as deposited, and (d) Ag(Cu) annealed at 600 °C.

and/or sublimation of the Ag and Ag(Cu) layers.[10,14] An important feature of Fig. 2 is that Ag(Cu) films show electrical behavior that is similar to that of pure Ag films, after annealing. Cu addition does not significantly increase the resistivity of the Ag films (after annealing).

Bragg-Brentano scans obtained from Ag and Ag(Cu) films are shown in Fig. 3. The scans contain information regarding the orientation of planes that are parallel to the substrate surface as well as any microstructural differences (e.g., lattice constant and strain) between the Ag and Ag(Cu) films. In the case of Ag films, all distinctive peaks [i.e., (111), (200), and (222) peaks] were enhanced after annealing at 600 °C for 1 h. On the other hand, in the case of Ag(Cu) films, (111) and (222) peaks were enhanced, whereas the (200) peak has almost vanished after annealing at 600 °C for 1 h.

Figure 4 shows relative intensities of (111) and (200) peaks for Ag and Ag(Cu) thin films on SiO_2 as obtained from θ-2θ scans (Fig. 3). Graphs above the break line are relative

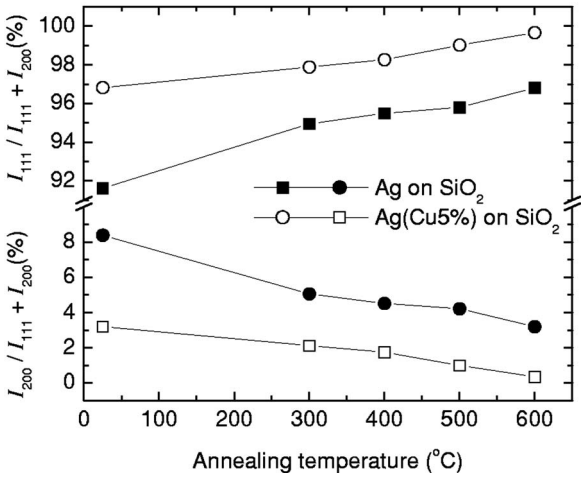

FIG. 4. Normalized (111) (plots over break line) and (200) (plots under break line) intensities measured by θ-2θ XRD scans for Ag and Ag(Cu) thin films as a function of the annealing temperature.

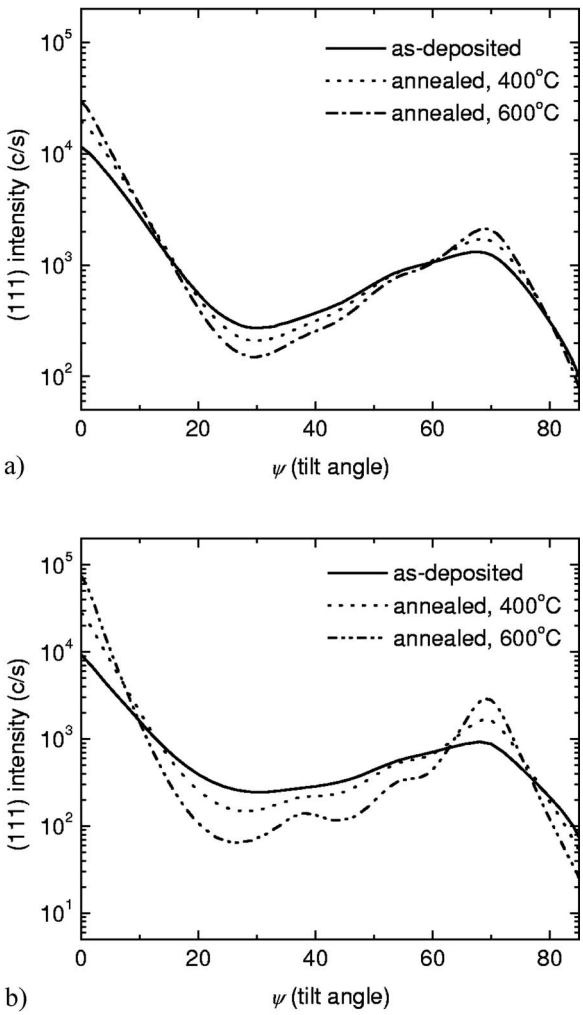

FIG. 5. (111) pole figure profiles for (a) Ag and (b) Ag(Cu) thin films, as deposited and annealed at 400 °C and 600 °C for 1 h in vacuum.

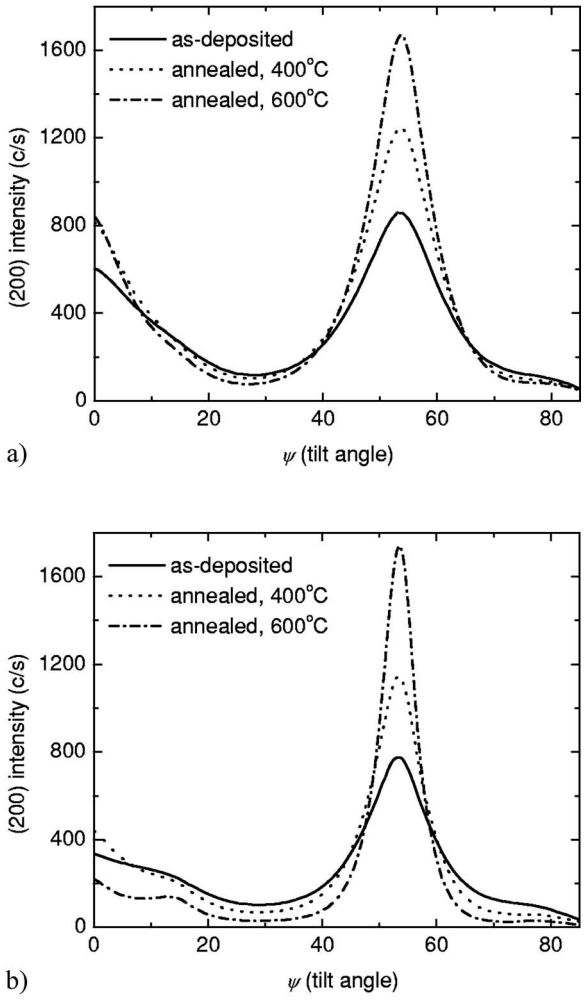

FIG. 6. (200) pole figure profiles for (a) Ag and (b) Ag(Cu) thin films, as deposited and annealed at 400 °C and 600 °C for 1 h in vacuum.

intensities of (111) normalized by (111) and (200) intensities. The (111) relative intensities from both Ag and Ag(Cu) thin films increase when the annealing temperature increases. This suggests a reduction in the (200) relative intensity as a function of annealing temperature. Typically, fcc metals such as Ag, Al, and Cu show [111] preferred orientation because the (111) plane has the lowest surface energy and the highest packing density.[11] However, the preferred orientation of an as-deposited thin film strongly depends on the film thickness,[10] deposition conditions,[11] and substrate types.[12] For the films deposited in this study, annealing enhances recrystallization and grain growth along the [111] direction by consumption of other grains having different crystallographic orientations.

Another important point from Fig. 4 is that the relative (111) intensities from the Ag(Cu) thin films were always higher than those from the Ag thin films over the entire annealing temperature range. (200) relative intensities from Ag films were always higher than those from Ag(Cu) films. Therefore, the θ-2θ XRD results indicate that Cu addition enhances [111] preferred orientation of the Ag thin films. To corroborate these findings, more detailed texture information was obtained from pole figure analysis.

Figure 5 shows pole figure profiles of (111) texture for Ag and Ag(Cu) thin films. At tilt angle $\psi=0°$, the (111) intensity is the highest for both samples. Another set of {111} planes is detected at $\psi=70.5°$ from the surface normal. Twin-related (511) texture[16] and (200) texture are also shown at $\psi=38.9°$ and 54.7°, respectively. The intensity of (111) texture in Ag and Ag(Cu) films increases with increasing annealing temperature. Furthermore, the background intensity for annealed samples becomes lower than that for as-deposited samples. Theoretically, the background intensity is related to the degree of random orientation.[16] Figure 5 indicates, therefore, that heat treatment enhances (111) texture for both samples. The enhancement of (111) texture can be quantitatively compared by measuring the half width at half maximum (HWHM).[17] The HWHMs of as-deposited and 600 °C annealed Ag thin films are 5.63° and 3.64°, respectively. In the case of Ag(Cu) thin films, the values decrease from 4.06° to 2.11° upon annealing at 600 °C. Because the lower HWHM represents a lower degree of random orientation, comparison of the Ag and Ag(Cu) HWHM values shows that Cu addition increases the degree of preferred orientation in the Ag(Cu) films.

Figure 6 presents (200) texture profiles from Ag and Ag(Cu) thin films annealed at different temperatures. The

TABLE I. Relative intensity of (200) peaks normalized by (111) intensity for Ag and Ag(Cu) thin films from Fig. 6.

	As deposited	400 °C	600 °C
Ag(Cu) on SiO_2	43.2%	38.4%	12.6%
Ag on SiO_2	70.3%	65.6%	50.4%

(200) and (111) peaks are shown at ψ (tilt angle)=0° and 54°, respectively. A distinct peak at ψ=15° in Fig. 6(b) corresponds to a twin-related (511) peak.[16] In the case of pure Ag films, the (200) intensity increases as a function of annealing temperature. In the case of Ag(Cu) films, however, the (200) intensity increases at 400 °C and then decreases at 600 °C. Table I lists the (200) relative intensity normalized by (111) intensity from (200) pole figure profiles. Note that the normalized (200) intensities of Ag films are higher than those of Ag(Cu) films over the entire temperature range. This signifies that the degree of (111) texture in Ag(Cu) films is higher than that in Ag films. The (200) intensity values decrease with increasing annealing temperature for both samples. The texture, however, evolves differently in each system. In the case of Ag thin films, the (111) and (200) textures evolve simultaneously. However, the (200) relative intensities appear to decrease when compared to (111) intensities because the increase of (111) intensity is greater than that of the (200) intensity for pure Ag layers. In the case of Ag(Cu), however, the (200) intensity decreases when the sample is annealed at 600 °C. This indicates that (200) oriented grains are consumed in favor of (111) grain growth during annealing. This result shows that Cu enhances (111) texture in Ag(Cu) thin films by consumption of non-{111} type grains, such as (200) oriented grains.

Figure 7 presents pole figure contour maps of (111) texture for as-deposited and 600 °C annealed samples. The (111) texture at the origin is dominant in both Ag and Ag(Cu) thin films. For both films, after annealing at 600 °C, the (111) peak at the origin becomes higher and sharper, indicating enhanced (111) texture. The narrower width of the peak

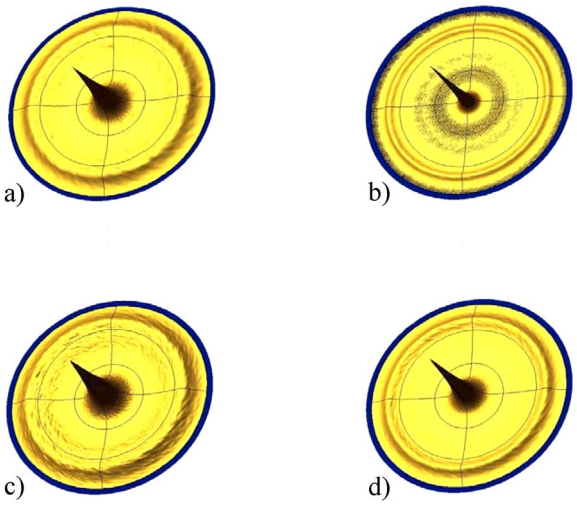

FIG. 7. (Color online) Three-dimensional contour plots of pole figures: (a) Ag(Cu) (111) as deposited, (b) Ag(Cu) (111) annealed at 600 °C, (c) Ag (111) as deposited, and (d) Ag (111) annealed at 600 °C.

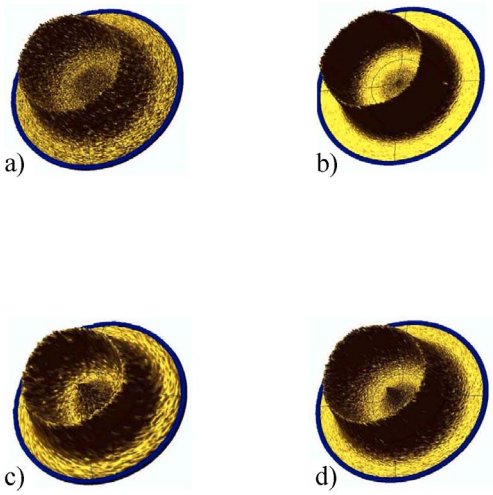

FIG. 8. (Color online) Three-dimensional contour plots of pole figures: (a) Ag(Cu) (200) as deposited, (b) Ag(Cu) (200) annealed at 600 °C, (c) Ag (200) as deposited, and (d) Ag (200) annealed at 600 °C.

for the Ag(Cu) thin film [Fig. 7(b), 4.22°] compared to that for the Ag thin film [Fig. 7(d), 7.28°] represents the effect of Cu resulting in texture enhancement of the Ag thin films.

The pole figure maps of (200) texture for Ag and Ag(Cu) thin films are shown in Fig. 8. These results are consistent with the texture profiles shown in Fig. 6. The (200) intensity at the origin, for the Ag(Cu) thin film, is almost absent after annealing at 600 °C while the (200) intensity from the Ag thin film still remains after heat treatment. In addition, since the fiber textured grains are randomly distributed about the surface normal (i.e., mosaic structure), ring type peaks appear on the contour plots. These ring type (200) intensities at ψ=54° are caused by diffraction from (200) planes of grains which have (111) planes parallel to the substrate surface.

Figures 9 and 10 show glancing angle XRD scans from Ag and Ag(Cu) thin films on SiO_2, respectively. Since the angle of incidence is fixed at 1° during the analysis (as shown in Fig. 1), the tilt angle of a specific {*hkl*} plane from the surface can be obtained using the following relation:

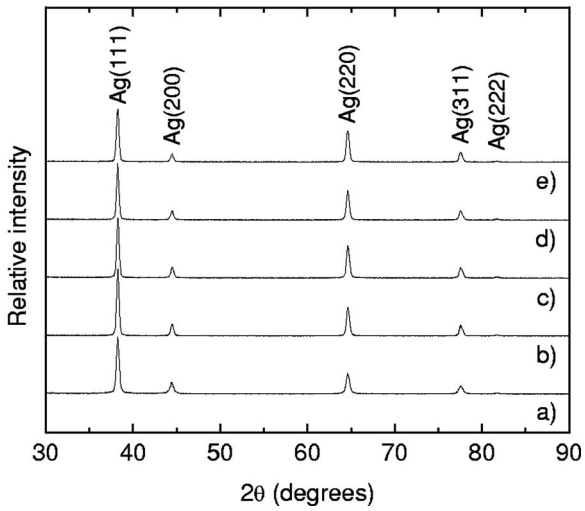

FIG. 9. Glancing angle x-ray diffraction profiles for Ag films: (a) as deposited and annealed at (b) 300 °C, (c) 400 °C, (d) 500 °C, and (e) 600 °C.

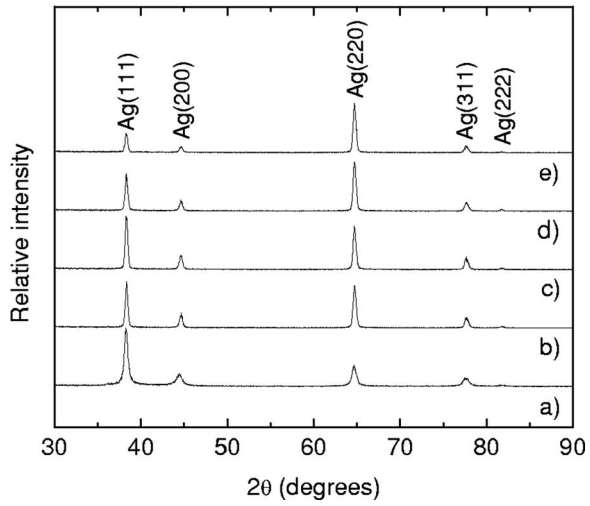

FIG. 10. Glancing angle x-ray diffraction profiles for Ag(Cu) films: (a) as deposited and annealed at (b) 300 °C, (c) 400 °C, (d) 500 °C, and (e) 600 °C.

$$\psi_{\{hkl\}} = \theta_b - \theta_g, \tag{1}$$

where θ_b is the angular peak position and θ_g is the incident angle. From texture analyses of Ag and Ag(Cu) thin films, it is evident that annealing enhances (111) texture by recrystallization or consuming other textures such as (200) or (220). As shown in Figs. 9 and 10, peak intensities from high index reflections such as (311) and (222) decrease as the temperature increases because these grains are consumed by the growth of (111) texture. The (220) peak intensity, however, increases as the annealing temperature increases.

This enhancement of the (220) peak (in the glancing angle XRD scans) can be understood based on the (111) texture evolution confirmed from Bragg-Brentano and pole figure analyses. Using Eq. (1) and (220) peak positions in Figs. 9 and 10, the angle, $\psi_{\{hkl\}}$; of the (220) plane is determined to be 31.5°. The theoretical angular difference between (111) and (220) planes is 35.2° which is 3.7° different from the measured value. Therefore, the (220) peaks in Figs. 9 and 10 come from those grains whose (111) plane normals are tilted 3.7° from the film-surface normal. Texture profiles in Fig. 5 show (111) enhancement at ψ=3.7° upon annealing. These data indicate that enhancement of (111) texture causes the increase of (220) intensity observed in glancing angle XRD scans. In addition, (111) intensities of Ag films (Fig. 9) are always higher than other intensities of peaks over the entire range of annealing temperatures, whereas the highest peak in Ag(Cu) films (Fig. 10) changes from (111) to (220) in Fig. 10(d). Therefore, it is inferred that (111) texture in Ag(Cu) film increases primarily by the consumption of other grains. The enhancement of (111) texture in Ag films, however, is attributed mainly to the recrystallization of disordered regions upon annealing[18] and not to the consumption of other grains with different crystallographic orientations.

Differences in surface morphology between Ag and Ag(Cu) films are presented in the AFM images in Fig. 11. Ag(Cu) film on SiO_2 [Fig. 11(a)] exhibits distinctive grooves at grain boundaries, whereas Ag films have dull edges between grains, as shown in Fig. 11(c). After the samples are annealed at 600 °C for 1 h, the surface of the Ag(Cu) film in Fig. 11(b) becomes smoother and small grains are incorporated into larger grains. Contrary to this, after annealing at 600 °C, Ag thin film [Fig. 11(d)] still maintains a surface structure similar to the as-deposited film [Fig. 11(c)].

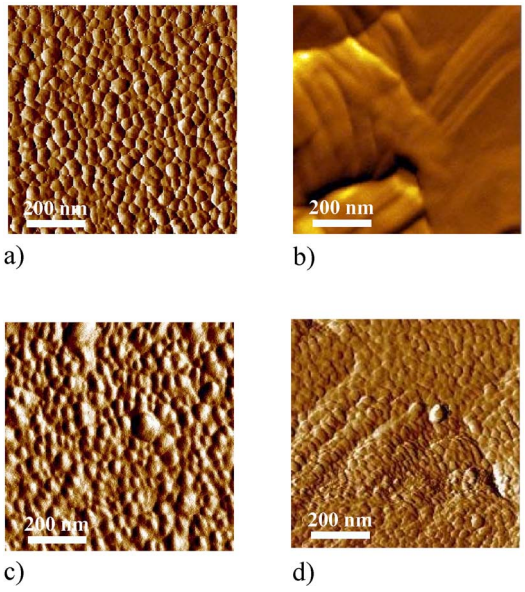

FIG. 11. (Color online) Atomic force microscopy images: (a) Ag(Cu) as deposited, (b) Ag(Cu) annealed at 600 °C, (c) Ag as deposited, and (d) Ag annealed at 600 °C thin films.

These morphological differences between Ag and Ag(Cu) films can be understood based on grain boundary grooving.[19] It has been reported that sharp grain boundary grooves are facilitated by enhanced surface diffusion.[19,20] The coefficient of adatom surface diffusion, based on a thermally activated process, is expressed by[21]

$$D^* = D_0 \exp\left(-\frac{E_m}{k_B T}\right), \tag{2}$$

where D_0 is the preexponential factor and E_m is the activation energy barrier. Grooves due to surface diffusion on Ag(Cu) thin film, are more distinctive when compared to pure Ag thin film, as shown in Figs. 11 and 12. It can be inferred that Cu addition lowers the activation barrier for Ag surface diffusion, thus generating the sharp grain boundaries in Ag(Cu) thin films.

Adatom surface diffusion is one of the kinetic factors which control microstructure evolution in polycrystalline films.[22] For low adatom diffusion, the microstructure becomes amorphous or nanocrystalline (small grains) because the adatoms do not have sufficient thermal energy for diffusion.[18] Given high adatom diffusion, however, the adatoms diffuse easily to generate sharp grooves between grains. High diffusion also enhances the degree of crystallinity and reduces the disordered regions between grains.[18,20]

The equilibrium grain boundary angle is given by[19]

$$\frac{\gamma_{gb}}{\gamma_s} = 2\cos\frac{\phi}{2}, \tag{3}$$

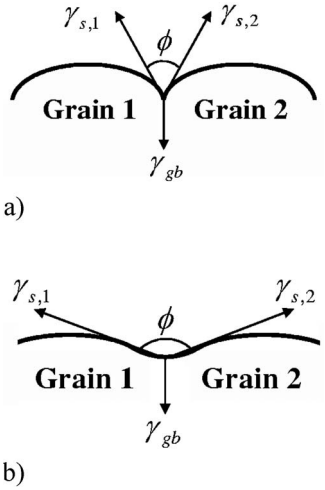

FIG. 12. Schematics of surface morphology: (a) Ag(Cu) as deposited and (b) Ag as deposited. γ_{gb} and γ_s are the grain boundary and surface energies per unit area, respectively. ϕ is the equilibrium angle between two surface energies.

where γ_{gb} is the grain boundary energy per unit area and γ_s is the surface energy per unit area. The change in grain boundary angle due to enhanced surface diffusion results in distinct grooves at grain boundaries to minimize the grain boundary energy of the thin film. The addition of Cu helps to reduce the amount of disordered borders between grains and results in enhanced texture of the Ag(Cu) thin film. It appears that for the case of as-deposited films, the increased (111) intensity from 91.6% to 96.8% is due to enhanced adatom diffusion by Cu addition.

IV. CONCLUSION

The texture evolution of Ag and Ag(Cu) thin films after annealing was investigated using Bragg-Brentano scan (θ-2θ geometry) and pole figure analyses. The analyses revealed that (111) textures of Ag and Ag(Cu) thin films were enhanced with increasing temperature up to 600 °C. Comparison of texture profiles between Ag and Ag(Cu) thin films showed that Cu addition enhanced Ag(Cu) (111) texture compared to that of pure Ag thin films. The enhanced (111) texture in Ag(Cu) thin films is due to Cu enhanced adatom diffusion. Glancing angle XRD results indicate different mechanisms for enhancement in (111) texture between Ag and Ag(Cu) films. Pure Ag films enhance (111) texture by recrystallizing disordered regions, whereas other oriented grains are consumed to enhance the (111) texture in the Ag(Cu) film. Comparison of surface morphologies between Ag and Ag(Cu) films indicates that Cu addition results in distinctive grain boundary grooving compared to pure Ag thin films.

ACKNOWLEDGMENTS

This work was partially supported by the National Science Foundation (L. Hess, Grant No. DMR-0602716) to whom the authors are greatly indebted. We acknowledge Professor J. Adams (ASU), D. C. Thompson (ASU), and Dr. N. D. Theodore (Freescale Semiconductor, Tempe, AZ) for discussion and critical review of the manuscript.

[1] C. V. Thompson, J. Floro, and H. I. Smith, J. Appl. Phys. **67**, 4099 (1990).
[2] L. Tang and G. Thomas, J. Appl. Phys. **74**, 5025 (1993).
[3] C. Detavernier and C. Lavoie, Appl. Phys. Lett. **84**, 3549 (2004).
[4] M. Zeitler, J. W. Gerlach, T. Kraus, and B. Rauschenbach, Appl. Phys. Lett. **70**, 1254 (1997).
[5] C. K. Hu, R. Rosenberg, and K. Y. Lee, Appl. Phys. Lett. **74**, 2945 (1999).
[6] D. B. Knorr and K. P. Rodbell, J. Appl. Phys. **79**, 2409 (1996).
[7] C. S. Hau-Riege and C. V. Thompson, Appl. Phys. Lett. **78**, 3451 (2001).
[8] E. M. Zielinski, R. P. Vinci, and J. C. Bravman, Appl. Phys. Lett. **67**, 1078 (1995).
[9] J. Cho and C. V. Thompson, Appl. Phys. Lett. **54**, 2577 (1989).
[10] H. C. Kim, T. L. Alford, and D. R. Allee, Appl. Phys. Lett. **81**, 4287 (2002).
[11] Y. S. Jung, Appl. Surf. Sci. **221**, 281 (2004).
[12] T. L. Alford, L. Chen, and K. S. Gadre, Thin Solid Films **429**, 248 (2003).
[13] M. Hauder, J. Gstottner, W. Hansch, and D. Schmitt-Landsiedel, Appl. Phys. Lett. **78**, 838 (2001).
[14] H. C. Kim, N. D. Theodore, and T. L. Alford, J. Appl. Phys. **95**, 5180 (2004).
[15] H. C. Kim, T. L. Alford, J. Appl. Phys. **94**, 5393 (2003).
[16] I. Tomov, M. Adamik, and P. B. Barna, Thin Solid Films **371**, 17 (2000).
[17] T. J. Klemmer, V. R. Inturi, and J. A. Barnard, J. Vac. Sci. Technol. A **15**, 1190 (1997).
[18] R. Knepper and R. Messier, Proc. SPIE **4467**, 87 (2001).
[19] W. W. Mullins, J. Appl. Phys. **28**, 333 (1957).
[20] C. E. Murray and K. P. Rodbell, J. Appl. Phys. **89**, 2337 (2001).
[21] J. Ferron, L. Gomez, J. J. de Miguel, and R. Miranda, Phys. Rev. Lett. **93**, 166107 (2004).
[22] C. V. Thompson, Annu. Rev. Mater. Sci. **30**, 159 (2000).